

# Nuclear-Magnetic-Resonance Echo Enhancement in an Antiferromagnet

Peter M. Richards

University of Kansas, Lawrence, Kansas

and

C. R. Christensen, B. D. Guenther, and A. C. Daniel  
 U. S. Army Missile Command, Redstone Arsenal, Alabama 35809  
 (Received 28 January 1971)

The observation of an anomalous enhancement of a two-pulse nuclear spin echo in antiferromagnetic MnO by a prepulse of variable width, amplitude, and delay time is described. A theory explaining this observation by adding frequency pulling to the Bloch equations is discussed. In this model the frequency pulling parameter is assumed to be inhomogeneous throughout the sample, consistent with current ideas of NMR line broadening in materials with strong pulling. Long free-induction decays observed following wide pulses are also explained.

## I. INTRODUCTION

The observation of an anomalous enhancement of spin echoes in the NMR of antiferromagnetic MnO has been reported.<sup>1</sup> The purpose of this paper is to examine this anomalous behavior in greater detail both experimentally and theoretically, and to relate it to other similar observed effects. Amplification of echoes has previously been observed for spin-wave resonances in ferrimagnetic yttrium iron garnet (YIG)<sup>2</sup> and for cyclotron resonances in plasmas.<sup>3</sup> A model describing echo amplification has been developed, and possible mechanisms for this effect in plasmas and in the electron-spin system of a ferrimagnet have been discussed.<sup>3-5</sup> We show here that the observed enhancement in the nuclear system is a natural consequence of frequency pulling combined with inhomogeneous broadening and we are able to explain several of the observed features. Although our results are directly applicable only to NMR, it is likely that similar effects are involved in the antiferromagnetic-resonance echoes.<sup>6</sup>

## II. EXPERIMENT

The spin echoes discussed in this paper were observed by placing a single crystal of MnO of approximately 10 mm<sup>3</sup> in a foreshortened reentrant cavity or a transmission line terminated by a helix. The echoes were excited by a pulsed triode oscillator producing 1.3 kW and/or by a pulsed signal generator producing 65 W. Sample shape and orientation were not important in obtaining our observed echo enhancement.

The typical spin-echo experiment is shown in Fig. 1(a). The pulse amplification experiment of Kaplan *et al.*<sup>2</sup> is shown in Fig. 1(b). We may think of this experiment in the following way: The first pulse of amplitude  $P_1$  is amplified, using the power in the second pulse, resulting in the echo of am-

plitude  $A_1$ . In the cyclotron echo experiment a two-pulse sequence is followed by a third pulse and the power in the third pulse is used to produce an amplified echo.

The parameters of the experiment to be described here are shown in Fig. 1(c). A spin echo pulse pair is preceded in a time  $t_3$  by a "prepulse" of width  $t_1$ . The prepulse, which changes the initial conditions in the spin echo experiment, is the source of the echo enhancement to be described below. The usual experimental arrangement was to produce the prepulse with the 65-W signal generator and the pulse pair with the 1.3-kW pulsed triode oscillator.

## III. RESULTS

Two Mn<sup>55</sup> nuclear magnetic resonances have been reported as shown in Fig. 2 for MnO in an external magnetic field.<sup>7</sup> The higher-frequency resonance  $\nu_H$  is only slightly field dependent, whereas the lower-frequency resonance  $\nu_L$  is strongly pulled to lower frequencies with decreasing field. Enhancement has been observed in both resonances.

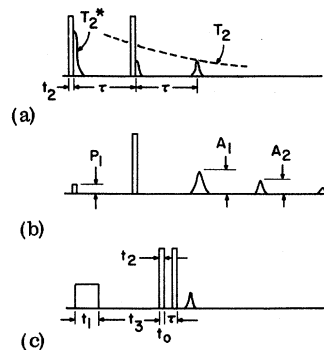


FIG. 1. Typical pulse sequences used in echo experiments. (a) Spin echo experiment, (b) pulse amplification experiment, (c) echo enhancement experiment.

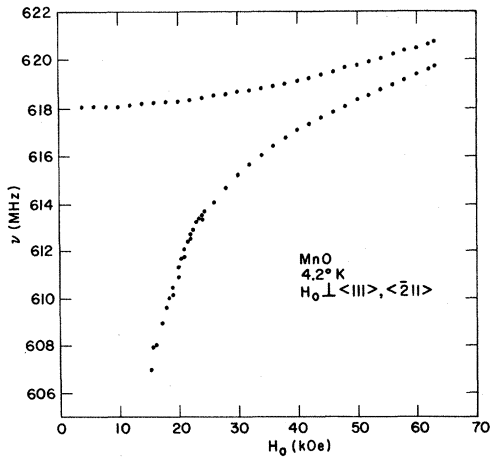


FIG. 2. Nuclear resonant modes in MnO at 4.2 K.

A recorder trace of the echo amplitude is shown in Fig. 3 for the  $\nu_H$  resonance as obtained from a boxcar integrator and as a function of the time separation  $t_3$  between the first pulse and the pulse pair. As  $t_3$  is increased, the echo amplitude increases rapidly to some maximum and then decreases to the amplitude obtained by the pulse pair. It was found from data, obtained with three pulses of equal power and width, that the initial increase could be described by an exponential with a characteristic time of no more than 13  $\mu\text{sec}$ . The decay of the echo amplitude was a simple exponential with a characteristic time of 165  $\mu\text{sec}$ , which is a factor of 20 longer than  $T_2$ . For these experiments  $T_2$  is defined as the decay of the echo amplitude with no prepulse and small values of  $t_2$ . Both of these times appear to be insensitive to large variations in the power or width of the prepulse but are dependent upon the applied magnetic field. The lower resonance  $\nu_L$  exhibited a more rapid decay with a characteristic time of about 80  $\mu\text{sec}$ .

The rapid increase and slow decrease of the echo amplitude is similar to the behavior of the pulse amplification observed in YIG. However, in YIG the echo amplitude exceeded that of the first pulse, whereas in this experiment the echo amplitude never approached the amplitudes of the applied pulses.

The echo enhancement was affected by varying the width  $t_1$  and the power of the prepulse. The behavior of the echo enhancement as a function of  $t_1$  is shown in Fig. 4 for  $\nu_H$  at several values of magnetic field  $H_0$ . These data were taken with the sample in a transmission line. When the sample was placed in a reentrant cavity, the enhancement went through a maximum as  $t_1$  was increased, and for very large values of  $t_1$  little or no enhancement was observed. In the transmission line, the rf fields were not as large as the fields produced in a

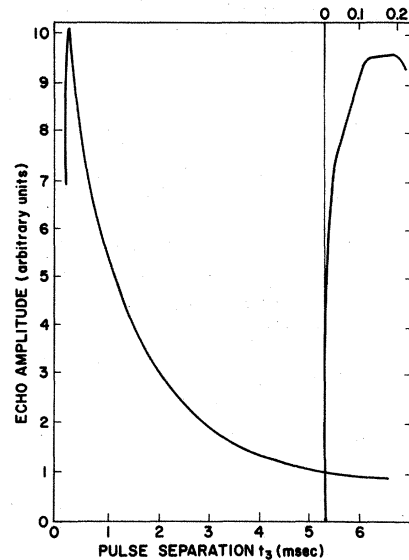


FIG. 3. Echo amplitude as a function of the pulse separation,  $t_3$ . The insert on the right is an expanded view of the initial increase in echo amplitude as  $t_3$  is increased from 0 to 0.2 msec.

reentrant cavity; this prevents the observation of maximum enhancement. Data similar to those shown in Fig. 4 were obtained for  $\nu_L$ . Interpretation of data obtained by varying  $t_1$  is complicated because both the frequency spectrum and the energy of the prepulse change with  $t_1$ . A more meaningful measurement is of echo power as a function of prepulse power with the prepulse width as a parameter. These effects are summarized in Figs. 5 and 6.

The power dependence of the echo enhancement exhibits a threshold characteristic as shown in Figs. 5 and 6. When the prepulse power is below a critical level, the signal is similar to that ob-

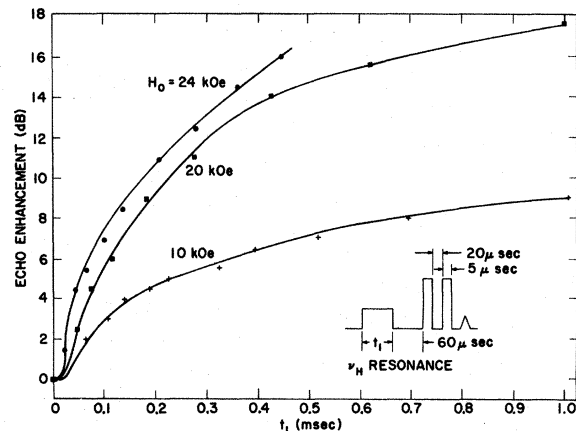


FIG. 4. Echo enhancement of the  $\nu_H$  resonance as a function of prepulse width  $t_1$  at three values of applied magnetic field.

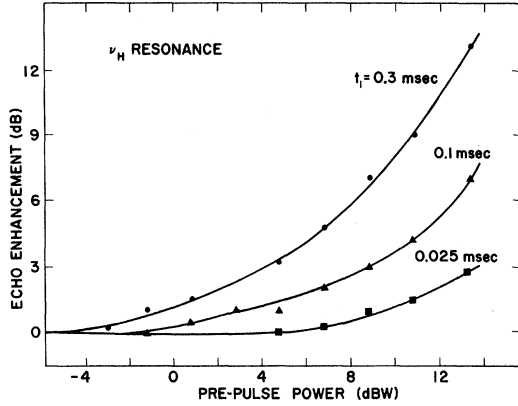


FIG. 5. Echo enhancement as a function of the pre-pulse power for the  $\nu_H$  resonance taken at 22 kOe.

tained from a simple nuclear-spin system with three exciting pulses. Above the threshold, the  $\nu_H$  echo enhancement increases slowly, appearing to have zero slope at threshold. The  $\nu_L$  echo enhancement has a linear power dependence above the threshold as shown in Fig. 6. A linear dependence is observed in the related cyclotron resonance experiments,<sup>3</sup> but without a threshold.

A long free-induction decay has been observed following the application of a long prepulse to  $\nu_H$ . This decay is shown in Fig. 7. The amplitude of the observed free-induction decay is much larger than the echo amplitude and is a function of the prepulse width and power.

#### IV. THEORY OF ECHO ENHANCEMENT

We propose a model which explains the salient features of the above results. It is based upon echo formation in a system, such as MnO, where there is strong pulling<sup>8</sup> of the NMR frequency.

Echoes have generally been described as falling into two main classes.<sup>5</sup> In the first class, referred to as a Hahn echo,<sup>9</sup> the natural frequency is independent of amplitude so that there is no intrinsic nonlinearity. However, for the gyromagnetic systems which exhibit this type of echo, the response to a large-amplitude pulse is nonlinear. Examples are NMR echoes where precession of real spins is involved, and photon echoes<sup>10</sup> in which the dipole moments behave gyromagnetically. The second class is caused by an intrinsic nonlinearity of the system, such as an amplitude-dependent frequency.<sup>4,5,11</sup> Ferrimagnetic<sup>5</sup> and cyclotron-resonance<sup>12</sup> echoes are believed to fall into this category. Henceforth we refer to these as type-2 echoes, as distinguished from the Hahn echoes.

##### A. NMR Echoes with Frequency Pulling

Reasonably large precession angles are obtainable for NMR in antiferromagnets, so that Hahn

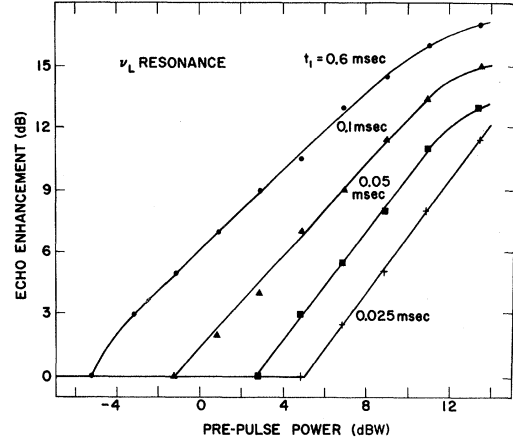


FIG. 6. Echo enhancement as a function of the pre-pulse power for the  $\nu_L$  resonance taken at 22 kOe.

echoes are possible, but in addition the frequency, expressed by<sup>8</sup>

$$\omega = \omega_n(1 - \gamma_e^2 A H_E I_z / \Omega^2), \quad (1)$$

is amplitude dependent.

Here,  $\omega_n$  is the unpulled frequency,  $A$  the hyperfine coupling constant,  $H_E$  the exchange field,  $\Omega$  the AFMR frequency,  $\gamma_e$  the electronic gyromagnetic ratio,  $I_z$  the expectation value of the nuclear spin  $I$  along its equilibrium direction  $z$ , and  $\gamma_e^2 A H_E I_z / \Omega^2 \ll 1$ . Since  $I_z$  depends on the precession angle or amplitude of transverse magnetization,<sup>12</sup> Eq. (1) provides the nonlinearity necessary for the type-2 echo.

To begin the development of the echo enhance-

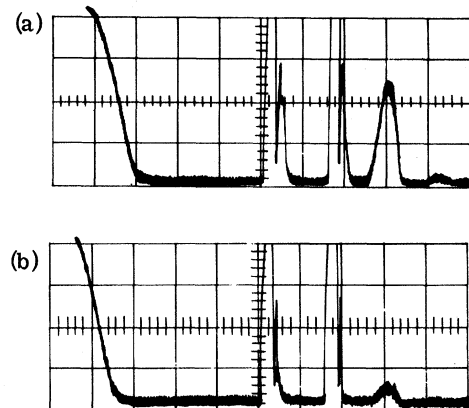


FIG. 7. Oscilloscope trace of the decay signal of  $\nu_H$  following a prepulse. The decay following the prepulse is driven to receiver saturation in order that the other decay signals may be observed. The scope x axis is 20  $\mu\text{sec}/\text{cm}$  and is triggered at the turnoff of the prepulse. The oscilloscope y axis is 0.5 V/cm.  $H_0 = 22$  kOe;  $\nu_H = 619.13$  MHz;  $t_2 = 1$   $\mu\text{sec}$ ;  $t_3 = 100$   $\mu\text{sec}$ ;  $\tau = 30$   $\mu\text{sec}$ . (a):  $t_1 = 800$   $\mu\text{sec}$ ; (b):  $t_1 = 200$   $\mu\text{sec}$ .

ment model, it is assumed that the pulling factor  $\gamma_e^2 A H_E I_z / \Omega^2$  is inhomogeneously broadened, as suggested by NMR linewidth studies on related compounds.<sup>13</sup> Thus, we write for the  $i$ th spin

$$\omega_i = \omega_n - \delta\omega_i z_i, \quad (2)$$

where

$$\delta\omega_i = \omega_n \gamma_e^2 A H_E \langle I_{iz} \rangle / \Omega_i^2, \quad (3)$$

$$z_i = I_{iz} / \langle I_{iz} \rangle. \quad (4)$$

Here  $\langle I_{iz} \rangle$  is the thermal equilibrium value of  $I_{iz}$  at the lattice temperature and the subscript on  $\Omega$  indicates that the source of inhomogeneous broadening is through the electronic frequencies.

An inhomogeneous distribution of  $\omega_n$  would not suppress the NMR echo, as is well known; however, here the inhomogeneities are contained in the amplitude-dependent part of the frequency. We show below that in such a case the inhomogeneous broadening *does* reduce the echo. Given this fact, the reason for echo enhancement by the prepulse is transparent: The prepulse increases nuclear-spin temperature and thus decreases  $z_i$  and the amount of inhomogeneous broadening. Hence, one expects the echo amplitude to be an increasing function of prepulse power.

To show the effect of the inhomogeneous pulling factor on the echo, it is necessary to have a quantitative description of echo formation. Difficulties in obtaining a solution of the NMR equations of motion under application of an rf pulse due to the nonlinearities can be reduced if we assume that the rf field  $H_1$  seen by the nucleus is sufficiently large that the precessional frequency in the rotating frame is  $\gamma_n H_1$  ( $\gamma_n$  is the nuclear gyromagnetic ratio) for the duration of the pulse. This will be the case if the spins initially are on resonance and the pulse time  $t_2$  is sufficiently short to prevent the system from being driven far off resonance. In this approximation, components of the nuclear magnetization following application of a pulse are given by the standard solution of the Bloch equations:

$$x_i(t_0 + t_2) = x_i(t_0), \quad (5a)$$

$$y_i(t_0 + t_2) = y_i(t_0) \cos \gamma_n H_1 t_2 + z_i(t_0) \sin \gamma_n H_1 t_2, \quad (5b)$$

$$z_i(t_0 + t_2) = -y_i(t_0) \sin \gamma_n H_1 t_2 + z_i(t_0) \cos \gamma_n H_1 t_2, \quad (5c)$$

in which the pulse field  $H_1$  is applied in the  $x$  direction of the rotating frame for a time  $t_2$  beginning at time  $t_0$  and  $x_i$  and  $y_i$  are normalized transverse components in the rotating frame defined as in Eq. (4). After application of the first pulse, the spins precess freely for a time  $\tau$ , so that we have

$$x_i(t_0 + t_2 + \tau) = x_i(t_0 + t_2) \cos \Delta\omega_i \tau e^{-\eta\tau}$$

$$+ y_i(t_0 + t_2) \sin \Delta\omega_i \tau e^{-\eta\tau}, \quad (6a)$$

$$y_i(t_0 + t_2 + \tau) = -x_i(t_0 + t_2) \cos \Delta\omega_i \tau e^{-\eta\tau} + y_i(t_0 + t_2) \sin \Delta\omega_i \tau e^{-\eta\tau}, \quad (6b)$$

$$z_i(t_0 + t_2 + \tau) = z_i(t_0 + t_2). \quad (6c)$$

Here we have included an intrinsic decay rate  $\eta$ . The frequency  $\Delta\omega_i$  is given by

$$\Delta\omega_i = \omega - \omega_i(t_0 + t_2), \quad (7)$$

where  $\omega$  is the driving (rotating frame) frequency and  $\omega_i(t_0 + t_2)$  is the resonance frequency of the  $i$ th spin at the end of the first pulse, hence the subscript 1 on  $\Delta\omega_i$ .

Following the free precession, a second pulse is applied at time  $t_0 + t_2 + \tau$  for duration  $t_2$ , and an echo is observed at a time  $\tau$  later in the usual way. The echo's amplitude is obtained by combining Eqs. (5) and (6) with similar equations for the magnetization following the second pulse and the second free precession period, respectively. It is important to note that  $\Delta\omega_{2i}$ , the frequency difference following the second pulse, is not equal to  $\Delta\omega_{1i}$  but instead is given by

$$\Delta\omega_{2i} = \Delta\omega_{1i} + \delta\omega_i z_0 (\alpha + \beta \cos \Delta\omega_i \tau), \quad (8)$$

where

$$\alpha = \cos \gamma_n H_1 t_2 (1 - \cos \gamma_n H_1 t_2), \quad (9)$$

$$\beta = \sin^2 \gamma_n H_1 t_2 e^{-\eta\tau}. \quad (10)$$

Here we have assumed the initial conditions  $x_i(t_0) = y_i(t_0) = 0$ ,  $z_i(t_0) = z_0$ . The term in  $\beta$  gives rise to the type-2 echo and hence represents a positive contribution of the frequency pulling to echo formation; however, the term in  $\alpha$ , which leads to suppression of the echo, outweighs the effect of  $\beta$ , and is responsible for the observed enhancement.

We assume a Gaussian distribution of  $\delta\omega$ 's centered at  $\delta\omega_0$ :

$$N(\delta\omega) \propto \exp[-(\delta\omega - \delta\omega_0)^2 / \sigma^2], \quad (11)$$

where  $\delta\omega_0$  is the pulling in the center of the NMR line and  $\sigma$  characterizes the width of the inhomogeneously broadened line. With suitable approximations, the echo enhancement is given by

$$S = z_0 e^{2(\tau/T)^2(1-z_0^2)}, \quad (12)$$

where  $T^{-2} = \frac{1}{4}\sigma^2(\alpha - \beta)^2$ . The enhancement  $S$  is defined as the ratio of echo power with a prepulse (the prepulse producing an initial magnetization  $z_0$ ) to the echo power with no prepulse ( $z_0 = 1$ ). Equation (12) is derived in Appendix A. Its validity requires  $\beta z_0 \delta\omega_0 \tau \gg 1$ . Since  $\delta\omega_0 \tau \approx 500$ , the condition roughly can be satisfied for pulse rotating angles  $\gamma_n H_1 t_2$  as small as  $6^\circ$  [see Eq. (10)].

The observed rate of decay of the echo amplitude is roughly given by  $\eta + T^{-1}$  (see Appendix A) in the absence of a prepulse, and thus  $T$  represents the measured transverse relaxation time if  $T^{-1} \gg \eta$ . An upper limit for the enhancement can be obtained by taking  $T^{-1} \ll \eta$  and picking the  $z_0$  which maximizes  $S$  for the experimental values of  $T$  and  $\tau$ . For  $\nu_H$ , the experimental numbers are  $\tau = 2 \times 10^{-5}$  sec and  $T = 11.7 \times 10^{-6}$  sec and  $6.5 \times 10^{-6}$  sec at 10 and 24 kOe applied fields, respectively (assuming the observed echo decay time is  $T$  as discussed above). These figures predict upper-limit enhancements of 17 and 72 dB at 10 and 24 kOe, respectively. For  $\nu_L$ , we have  $\tau = 8 \times 10^{-6}$  sec and  $T = 2 \times 10^{-6}$  sec, nearly independent of field, giving an upper-limit enhancement of 128 dB which is considerably greater than the largest observed enhancement of 15 dB. Reference to Figs. 5 and 6 shows that the observed enhancements are well within these upper limits. Note also that the enhancement of  $\nu_H$  is an increasing function of applied field, as suggested by the above numbers.

#### B. Specialization to NMR Modes in MnO

The preceding has demonstrated that echo enhancement can occur owing to frequency pulling and that the observed enhancements fall well below the calculated upper limits. The analysis has tacitly assumed only one NMR mode as in a ferromagnet, whereas two modes are present in MnO (Fig. 2), and echo enhancement is observed at driving frequencies corresponding to resonance of each of them. These modes are qualitatively different in regard to frequency pulling, as discussed below. Nonetheless, it is reasonable to expect enhancement when pumping either at  $\nu_H$  or  $\nu_L$ , as we shall describe.

Our basic premises are that (a) only the low-frequency mode  $\nu_L$  shows appreciable pulling and (b) only  $\nu_L$  produces a measurable echo, so that even when the pumping frequency is  $\nu_H$ , the observed echo is actually due to the off-resonance excitation of the  $\nu_L$  mode. The justification for (a) is discussed elsewhere.<sup>14</sup> Given that  $\nu_H$  is unpulled, we are led to (b) for the following reasons: A sizable echo is possible only if the homogeneous broadening is less than the inhomogeneous broadening. The well-defined nuclear spin-wave spectrum associated with a strongly pulled mode has been shown<sup>15</sup> to reduce the intrinsic width of the NMR line considerably below the Suhl-Nakamura<sup>16</sup> value so that the observed width is most likely due to inhomogeneous broadening of the pulling factor, as in Eq. (3). For a mode with negligible pulling, the situation is reversed; inhomogeneous broadening is reduced and one should observe the full Suhl-Nakamura width.

We therefore assert that the echo enhancement

is given by Eq. (12) with parameters appropriate to the  $\nu_L$  resonance, regardless of whether the driving frequency is in the vicinity of  $\nu_H$  or  $\nu_L$ . When referring to the "echo of the  $\nu_H$  resonance" as in Sec. III, we mean that the applied frequency is near  $\nu_H$ .

Consider first the  $\nu_L$  echo. Here Eq. (12) and the approximations leading to it should be essentially correct since the  $\nu_L$  mode is on resonance before application of any of the pulses. The observed enhancement of 15 dB is way below the upper limit of 128 dB. This can be explained simply by noting that the upper limit occurs when  $z_0 = 0.125$  (we use  $\tau = 8 \times 10^{-8}$  sec,  $T = 2 \times 10^{-6}$  sec, as before), i. e., the prepulse would increase the nuclear-spin temperature by a factor of 8. An increase of nuclear-spin temperature of this magnitude would throw the mode well off resonance and inhibit rf absorption. A value  $z_0 = 0.94$  gives the observed 15-dB enhancement when inserted into Eq. (16). This modest 6% increase of nuclear-spin temperature is likely all that one should expect if the driving frequency is  $\nu_L$ .

The  $\nu_H$  echo, defined in the sense stated above, is observed when the pumping frequency is  $\nu_H = \omega_n/2\pi$ . Although the  $\nu_H$  mode does not produce an echo, it does absorb energy from the driving field. In particular, a small  $z_0$  (large nuclear-spin temperature) can now be produced by the prepulse since the  $\nu_H$  resonance frequency is independent of amplitude. As  $z_0$  is decreased, the resonance frequency of the  $\nu_L$  mode approaches the pumping frequency. This fact gives an additional source of echo enhancement since application of a prepulse will bring  $\nu_L$  closer to resonance. Thus the mechanism described by Eq. (12) may not be necessary to explain the existence of enhancement when the driving frequency is  $\nu_H$ , but it does seem to be the controlling factor for the  $\nu_L$  enhancement.

We also note that the parameters  $\alpha$  and  $\beta$  which are related to change of  $z$  between pulses will be different for pumping at  $\nu_L$  and  $\nu_H$  because coupling of the rf to the two modes is different. Since  $T$  depends on  $\alpha$  and  $\beta$ , we therefore do not expect it to be the same for both  $\nu_H$  and  $\nu_L$  echoes.

The fact that the observed echo decay time for  $\nu_H$  is about four times larger than for  $\nu_L$  may have nothing to do with intrinsic decay rates of the two modes but could be due to the fact that  $\alpha$  and  $\beta$  are less for  $\nu_H$ . The  $\nu_L$  resonance is stronger than  $\nu_H$  at the dc fields of interest, which is consistent with larger  $\alpha$  and  $\beta$  for  $\nu_L$ .

#### C. Dependence of Enhancement on $t_3$

Dependence of echo enhancement upon the time  $t_3$  between the prepulse and start of the pulse pair (Fig. 1) should be obtained simply from the dependence of  $z_0$  on  $t_3$ , which we take as

$$z_0 = 1 - (1 - z_p) e^{-t_3/T_1}, \quad (13)$$

where  $z_p$  is the value at the end of the prepulse. According to Eq. (12) this would predict that as  $t_3$  increases, enhancement would both increase toward maximum and decrease from maximum with a characteristic time of the order of  $T_1$  (see Fig. 3). For  $t_3 > (t_3)_{\max}$ , where  $(t_3)_{\max}$  is the value of  $t_3$  at maximum enhancement,  $S$  decreases with a time constant of about 200  $\mu\text{sec}$ , which is reasonable for an NMR  $T_1$  in an antiferromagnet.<sup>17</sup>

For times  $t_3 < \tau$ , however,  $S$  increases with a characteristic time of the order of 10  $\mu\text{sec}$ , which is much too short on the basis of Eqs. (12) and (13). With times  $t_3$  less than the pulse-pair separation  $\tau$ , one can no longer assume that the only effect of the prepulse is to change the nuclear-spin temperature. Components of transverse magnetization resulting from the prepulse will not have had time to decay out as long as  $t_3 \lesssim \eta^{-1}$ , and since  $\tau \lesssim \eta^{-1}$ , in order for a sizable echo to appear, the situation  $t_3 < \tau$  implies nonzero transverse magnetization (for the  $i$ th spin) at the beginning of the pulse pair. One can show that, for the normal Hahn echo, remnant transverse magnetization at  $t=0$  has no effect on the echo at  $2\tau + 2t_2$  as long as  $t_3$  and  $\tau$  are not integer multiples of each other. The amplitude-dependent frequency does cause a reduction in the echo owing to the transverse components at  $t=0$ , as we show below.

If there is nonzero transverse magnetization at the beginning of the pulse pair, then Eq. (8) contains additional terms and becomes

$$\begin{aligned} \Delta\omega_{2i} = & \Delta\omega_{1i} + \delta\omega_i z_0 (\alpha + \beta \cos \Delta\omega_{1i} \tau) \\ & + \delta\omega_i [a \cos(\Delta\omega_{0i} t_3 + \theta_a) + b \cos(\Delta\omega_{0i} t_3 + \Delta\omega_{1i} \tau + \theta_b) \\ & + c \cos(\Delta\omega_{0i} t_3 - \Delta\omega_{1i} \tau + \theta_c)], \quad (14) \end{aligned}$$

where  $\Delta\omega_{0i}$  is the value for  $\Delta\omega_i$  during the interval after the prepulse and before the pulse pair,  $\theta_a$ ,  $\theta_b$ , and  $\theta_c$  are appropriate phase angles, and

$$a = -\sin\gamma_n H_1 t_2 (1 - \cos\gamma_n H_1 t_2) (x_p^2 + y_p^2)^{1/2} e^{-\eta t_3}, \quad (15a)$$

$$b = -\frac{1}{2} \sin\gamma_n H_1 t_2 (1 + \cos\gamma_n H_1 t_2) (x_p^2 + y_p^2)^{1/2} e^{-\eta(t_3 + \tau)}, \quad (15b)$$

$$c = -\frac{1}{2} \sin\gamma_n H_1 t_2 (1 - \cos\gamma_n H_1 t_2) (x_p^2 + y_p^2)^{1/2} e^{-\eta(t_3 + \tau)} \quad (15c)$$

for the approximations made earlier, where  $x_p$  and  $y_p$  are components of transverse magnetization at the end of the prepulse. The quantities  $a$ ,  $b$ , and  $c$  arise from effects of the initial transverse magnetization on the difference  $z_1 - z_2$  between  $z$  components following the first and second pulses of the pulse pair. Equation (6) has been used to

relate  $x_0$  and  $y_0$  to their values at the end of the prepulse.

We see that the initial transverse magnetization gives additional frequency components to  $\Delta\omega_{2i} - \Delta\omega_{1i}$ , and thus further reduces the echo. Details of the reduction are given in Appendix B. Since  $a$ ,  $b$ , and  $c$  go to zero as  $e^{-\eta t_3}$ , it is evident that the characteristic time over which the echo increases with  $t_3$  is of the order of  $\eta^{-1} \ll T_1$ . The actual dependence of echo amplitude upon  $t_3$  for  $t_3 \lesssim \eta^{-1}$  is complicated (see appendices), so it may be risky to attempt to infer anything other than an order-of-magnitude estimate for  $\eta$  from the observed echo buildups for short  $t_3$ .

Additional echoes appear for  $t_3 \leq \tau$  since now, for example, the prepulse and the first pulse may be regarded as a pulse pair and produce an echo at a time  $t_3$  following the first pulse. The additional echoes have been observed for very small values of  $t_3$ .

#### V. FREE-INDUCTION DECAY FOLLOWING PREPULSE

Free-induction decay after the prepulse has also been observed (Fig. 7) with time constants of about  $5 \times 10^{-6}$  sec. Similar effects were reported by Mahler and James<sup>18</sup> for  $\text{KMnF}_3$ . We believe this occurs as the result of steady-state saturation reducing the inhomogeneous broadening effectively to zero. The steady-state condition under application of a long rf pulse is one in which all spins which absorb power have the same resonance frequency regardless of the spread in  $\delta\omega_i$ 's. This may be seen in terms of a rate equation for absorption of rf by the pulled mode:

$$\frac{dz_i}{dt} = -W_i z_i + \frac{(1 - z_i)}{T_1}, \quad (16)$$

where  $W_i$  is the rf transition probability for the  $i$ th spin. Steady-state solution gives

$$z_i = (1 + W_i T_1)^{-1}. \quad (17)$$

But owing to the dependence of resonance frequency upon  $z_i$ ,  $W_i$  is itself a function of  $z_i$ . We have

$$W_i = p_L [1 + (\omega_n - \omega \delta\omega_i z_i)^2 / \eta^2]^{-1} + p_H [1 + (\omega_n - \omega)^2 / \eta^2]^{-1}, \quad (18)$$

where  $p_L$  and  $p_H$  represent, respectively, coupling to the low- and high-frequency modes and are each proportional to the rf power. For sufficiently large power and  $\delta\omega \gg \eta$ , a simultaneous solution of Eqs. (17) and (18) is possible for which  $\delta\omega_i z_i \approx \omega_n - \omega$ , provided  $\delta\omega_i > \omega_n - \omega$ . The situation is similar to that discussed by De Gennes *et al.*<sup>8</sup> in their treatment of steady-state behavior, and the features of a graphical solution to Eqs. (17) and (18) may be found in their paper. The second term in Eq. (18) makes no fundamental change, but an important difference is that we explicitly account for inhomog-

eneous broadening by treating each spin, or group of spins with the same resonance frequency, as an independent oscillator with its own  $W_i$ . We believe this to be a more accurate approach since  $\sum_i W_i z_i \neq \bar{z} \sum_i W_i$ , where  $\bar{z}$  is the spatial average of  $z_i$ . The calculation of Ref. 8 implicitly assumes the two quantities to be equal.

If rf saturation is carried out at a frequency  $\omega > \omega_n - \delta\omega_0 + \sigma$ , then all parts of the inhomogeneously broadened line will be brought on to resonance with the same resonance frequency. This equality of resonance frequencies and hence lack of inhomogeneous broadening will persist after the pulse as long as the individual  $z$  components maintain their values. For an inhomogeneous spread of  $\delta\omega$ 's, we require a nonuniform distribution of  $z$ 's in order to achieve the above condition. Hence the state of rf saturation is one of nonuniform nuclear-spin temperature throughout the sample. Once a finite uniform spin temperature is attained, the inhomogeneous broadening returns, and the free-induction decay rapidly disappears. In the absence of intrinsic damping,  $\eta \rightarrow 0$ , we would thus identify the observed free-induction decay time following a relatively long saturating pulse as the time required for elimination of spin temperature gradients.

If the spin temperature obeys a diffusion equation, and the characteristic distance over which  $\delta\omega$  (and thus  $z$  in the condition of cw saturation) varies is  $r_0$ , then we expect to have

$$\tau_D \approx r_0^2/D, \quad (19)$$

where  $D$  is the diffusion constant and  $\tau_D$  is the characteristic time for reaching a uniform temperature distribution. The methods of Bennett and Martin<sup>19</sup> as extended by McFadden and Tahir-Kheli<sup>20</sup> may be used to estimate  $D$ . The latter authors have evaluated moments which may be applied to a transverse, long-range interaction such as the Suhl-Nakamura one. With some manipulation we may express their results as

$$D = \frac{1}{12} \sqrt{\pi} R_0^2 \langle \Delta\omega^2 \rangle_{SN}^{1/2}, \quad (20)$$

where  $R_0$  is the range of the Suhl-Nakamura interaction, and  $\langle \Delta\omega^2 \rangle_{SN}$  is the second moment of the NMR line due to the Suhl-Nakamura interaction. For the spin-wave spectrum<sup>21</sup> of MnO and an applied field of 24 kOe along  $\langle 100 \rangle$ , we estimate  $R_0 \approx 200 \text{ \AA}$  and  $\langle \Delta\omega^2 \rangle_{SN}^{1/2} \approx 3.5 \times 10^6 \text{ sec}^{-1}$ . A representative value for  $r_0$  may be  $5 \times 10^{-5} \text{ cm}$  which, combined with the above figures and Eqs. (4) and (5), gives  $\tau_D \sim 10^{-3} \text{ sec}$ .

The observed free-induction decay time in this situation would be  $\eta^{-1}$  since  $\eta \gg 1/\tau_D$  for such a long  $\tau_D$ . On the other hand, if  $r_0 \approx R_0$  so that the inhomogeneity and Suhl-Nakamura ranges are comparable, then  $\tau_D \approx 2 \times 10^{-6} \text{ sec}$  and the free-induction

decay would probably be limited by  $\tau_D$ .

The long free-induction decay occurs when pumping at  $\nu_H$  but does not appear on the  $\nu_L$  resonance. This is consistent with the above arguments since, when pumping at  $\nu_L$ , the condition  $\omega > \omega_n - \delta\omega_0 + \sigma$  is not met and the inhomogeneous broadening remains.

## VI. SUMMARY

Echo enhancement has been observed for both the high- and low-frequency NMR modes in antiferromagnetic MnO. Enhancement is defined as an increase in echo power upon application of a prepulse over its value in the absence of the prepulse. This enhancement occurs for the time between the prepulse and the echo-producing pulse pair sufficiently long that the only effect of the prepulse should be to increase the nuclear-spin temperature.

We have considered echo formation for NMR in antiferromagnets where there is strong frequency pulling. Here one has both the gyromagnetic response associated with a Hahn echo and the amplitude-dependent frequency characteristic of the type-2 echo. When both these effects are accounted for, we are able to explain the observed echo enhancement semiquantitatively. The basic feature of the explanation is that the major source of inhomogeneous broadening occurs in the frequency pulling  $\delta\omega_i z_0$ , and inhomogeneous broadening in this form tends to decrease the echo. As the nuclear-spin-temperature increases, the frequency pulling decreases and the echo is less adversely affected by the inhomogeneities. The resulting enhancement is most transparently displayed by Eq. (12).

Anomalous long free-induction decays are observed following a prepulse at the high-frequency resonance. This is also explained by the model of inhomogeneous frequency pulling.

## VII. CONCLUSIONS

Several features of the observed echo enhancement can be explained in terms of frequency pulling and inhomogeneous broadening, as we have shown. Numerical estimates are difficult because of uncertainties regarding the intrinsic relaxation rate and precise behavior of the transverse magnetization during application of an rf pulse when both frequency pulling and damping are present. Nonetheless, it is possible to establish an upper limit for the enhancement, and observed enhancements fall well below this. Thus, it appears that enhancement can be interpreted within the framework of this model without any new mechanisms having to be introduced.

An unresolved problem is the dependence of echo enhancement on prepulse power. It is evident that enhancement is a function of this power since nuclear-spin temperature should increase with increasing pulse power and duration. Also, it is not

difficult to see that dependence can be different for enhancement at the two different mode frequencies. Equation (18) shows that for  $\omega \approx \omega_n$ , corresponding to  $\nu_H$ , the rf transition probability is constant for small  $z_i$  and increases as nuclear-spin temperature increases. When pumping at  $\nu_L$ , however,  $W_i$  depends strongly on  $z_i$  since the system is thrown off resonance as spin temperature increases.

In the case of pumping at  $\nu_L$  it is not possible to change  $z_i$  appreciably as long as  $\omega_n$  stays constant. The approximate solution to Eqs. (17) and (18) is

$$z_i \approx (\omega_n - \omega) / \delta \omega_i \quad (21)$$

for  $\omega_n - \omega \approx \delta \omega_i \gg \eta$ . If  $\omega = 2\pi\nu_L \approx \omega_n - \delta \omega_i$ , then the nuclear-spin temperature does not increase, and no enhancement would be observed. This is consistent with the observation that no enhancement of the  $\nu_L$  echo is seen for powers below a critical level  $P_c$ . The quantities  $\omega_n$  and  $\delta \omega_i$  are functions of the sublattice magnetization  $\langle S_z \rangle$ , which is dependent on the lattice temperature. If we assume that lattice heating occurs only via rf energy input from the nuclear-spin system (no direct coupling of the rf to the lattice), then we have  $\omega_n = \omega_n(z_i)$ ,  $\delta \omega_i = \delta \omega_i(z_i)$ . Putting this into Eq. (21) leads to an equation for  $z_i$  which has, as well as  $z_i \approx 1$ , a root for which  $z_i < 1$ . The root  $z_i < 1$  occurs only above the critical power  $P_c$  since Eq. (17) must also be satisfied. Hence, this model predicts a sudden jump in nuclear-spin temperature at a critical power and practically no change until  $P_c$  is reached. Above  $P_c$ , there is essentially no further change in nuclear-spin temperature. This behavior is familiar in the double-resonance experiments.<sup>22</sup>

The discrepancy between this model and experiment for the  $\nu_L$  echo enhancement is that experiment shows a linear increase in enhancement as  $P$  is increased above  $P_c$  with no discontinuity at  $P_c$ . If we allow direct coupling of rf to the lattice so that  $\omega_n$  and  $\delta \omega_i$  can change without resonant absorption of energy by the nuclear spins, then we find a gradual increase of nuclear temperature with power, but the threshold effect is lost.

#### APPENDIX A: DERIVATION OF EQ. (12)

The general expression for a transverse component of the  $i$ th spin at the echo time is of the form

$$x_i(t_0 + 2\tau + 2t_2) = \sum_{m=-1}^1 \sum_{n=-1}^1 a_{mn} e^{-\eta(|m|+|n|)\tau} \times e^{i(m\Delta\omega_{1i} + n\Delta\omega_{2i})\tau}, \quad (A1)$$

where the coefficient  $a_{mn}$  may be determined from Eqs. (5) and (6) as discussed in the text. Since  $\Delta\omega_{2i}$  is a function of  $\tau$  by Eq. (8), Eq. (A1) does not show explicitly all the Fourier components.

The complete Fourier decomposition is made by using Eq. (8) together with the expansion<sup>23</sup>

$$e^{i\alpha \cos \varphi} = \sum_n (-i)^n J_n(\alpha) e^{in\varphi}$$

in terms of Bessel functions  $J_n$ . The bulk  $x$ -component magnetization is proportional to  $\sum_i x_i$ , and we assume that all terms with a net Fourier component at a nonzero multiple of  $\Delta\omega_{1i}$   $\tau$  vanish because of the inhomogeneous broadening. The result for transverse components at the echo time then is

$$\sum_i x_i = z_0 \sum_i \{ [\lambda_0 J_0(\beta \delta \omega_i z_0 \tau) + \lambda_2 J_2(\beta \delta \omega_i z_0 \tau)] \times \sin \alpha \delta \omega_i z_0 \tau + \lambda_1 J_1(\beta \delta \omega_i z_0 \tau) \cos \alpha \delta \omega_i z_0 \tau \}, \quad (A2)$$

$$\sum_i y_i = z_0 \sum_i \{ [\lambda_0 J_0(\beta \delta \omega_i z_0 \tau) + \lambda_2 J_2(\beta \delta \omega_i z_0 \tau)] \times \cos \alpha \delta \omega_i z_0 \tau - \lambda_1 J_1(\beta \delta \omega_i z_0 \tau) \sin \alpha \delta \omega_i z_0 \tau \}, \quad (A3)$$

where

$$\lambda_0 = -\frac{1}{2} \sin \gamma_n H_1 t_2 (1 - \cos \gamma_n H_1 t_2) e^{-2\eta\tau}, \quad (A4)$$

$$\lambda_1 = \frac{1}{2} \sin 2\gamma_n H_1 t_2 e^{-\eta\tau}, \quad (A5)$$

$$\lambda_2 = -\frac{1}{2} \sin \gamma_n H_1 t_2 [1 + \cos \gamma_n H_1 t_2] e^{-\eta\tau}, \quad (A6)$$

and  $J_0$ ,  $J_1$ , and  $J_2$  are Bessel functions. In (A2) we have also assumed  $\alpha \delta \omega_i z_0$ ,  $\beta \delta \omega_i z_0 \ll \Delta\omega_{1i}$  so that no nonnegligible dc components arise when a Fourier component is a multiple of  $\alpha \delta \omega_i z_0$  or  $\beta \delta \omega_i z_0$ . This is justifiable for a small pulse precession angle  $\gamma_n H_1 t_2$  and can be consistent with the discussion following Eq. (12).

Integrations over the Gaussian distribution of Eq. (11) may be performed without difficulty in the limits  $\beta \delta \omega_0 z_0 \tau \ll 1$  and  $\beta \delta \omega_0 z_0 \tau \gg 1$  by using appropriate expansions<sup>23</sup> for the Bessel functions. The results are

$$x^2 + y^2 = N^2 z_0^2 e^{-\alpha^2 \sigma^2 z_0^2 \tau^2} / 2 \{ [\lambda_0 + \frac{1}{8} \lambda_2 \beta^2 \delta \omega_0^2 z_0^2 \tau^2] + \frac{1}{4} \lambda_1^2 \beta^2 \delta \omega_0^2 z_0^2 \tau^2 \} \quad \text{for } \beta \delta \omega_0 z_0 \tau \ll 1, \quad (A7)$$

$$x^2 + y^2 = N^2 (2\pi \beta \delta \omega_0)^{-1} z_0 \{ (\lambda_0 - \lambda_2 + \lambda_1)^2 e^{-\sigma^2 z_0^2 (\alpha + \beta)^2 / 2} + (\lambda_0 - \lambda_2 - \lambda_1)^2 e^{-\sigma^2 z_0^2 (\alpha - \beta)^2 / 2} + [(\lambda_0 - \lambda_2)^2 - \lambda_1^2] \times \sin 2\delta \omega_0 \tau_2 e^{-\sigma^2 z_0^2 \tau^2 (\alpha^2 + \beta^2) / 2} \} \quad \text{for } \beta \delta \omega_0 z_0 \tau \gg 1, \quad (A8)$$

where  $N$  is the total number of spins and we have assumed  $\sigma \ll \delta \omega_0$ . The quantity  $x^2 + y^2$  is proportional to the square of the net transverse magnetization and thus to the power radiated by the echo.

Equation (A8) ( $\beta \delta \omega_0 z_0 \tau \gg 1$ ) should be appropriate to most of the region of interest. This can be seen from the facts that sizable enhancement must come from the exponentials (enhancement requires  $x^2 + y^2$

to increase as  $z_0$  decreases) and that  $\sigma \ll \delta\omega_0$ . Thus, if  $\alpha$  and  $\beta$  are comparable in magnitude, the condition  $\beta\delta\omega_0 z_0 \tau \gg 1$  is mandatory for enhancement. For example, if  $\eta\tau \ll 1$  and  $\omega_p t_2 \gg 1$ , we have  $\beta = 2\alpha$ . For simplicity we assume  $\alpha z_0 \sigma \tau, \beta z_0 \sigma \tau > \sqrt{2}$  so that one exponential dominates and the oscillations are negligible. The result is then Eq. (12).

Note that the observed rate of echo decay contains  $\eta$  through the parameters  $\lambda_0, \lambda_1, \lambda_2$ , and  $\beta$ . Depending on the relative sizes of  $\lambda_0, \lambda_1$ , and  $\lambda_2$ , the characteristic decay rate for the echo amplitude is between  $\frac{1}{2}\eta + T^{-1}$  and  $\frac{3}{2}\eta + T^{-1}$ .

#### APPENDIX B: ECHO FOR $t_3 < \tau$

Equation (A1) still holds in this case (with a modified  $a_{mn}$ ), but  $\Delta\omega_{2i}$  is given by the more complex Eq. (14) rather than Eq. (8) which neglects initial transverse magnetization. The same arguments

which lead from Eq. (A1) to (A2) and (A3) should now be multiplied by  $J_0(\delta\omega_i a) J_0(\delta\omega_i b) J_0(\delta\omega_i c)$  and other combinations of three Bessel functions resulting from Fourier components that do not contain the phase  $\Delta\omega_{0i} t_3$ .

There are competing effects in the initial transverse components  $x_0, y_0$  which tend to cause an increase in echo amplitude. These arise from terms of the form

$$y_0 e^{i(\Delta\omega_i \pm \Delta\omega_2)\tau}$$

which can have a dc component as a result of Eq. (14). Such dc components, however, require products of four Bessel functions, at least one of which must be of nonzero order. Because of this, we assume these terms to be small compared with the previously mentioned ones which cause a decrease in echo amplitude.

<sup>1</sup>C. R. Christensen, B. D. Guenther, and A. C. Daniel, *Bull. Am. Phys. Soc.* **14**, 1185 (1969).

<sup>2</sup>D. E. Kaplan, R. M. Hill, and G. F. Herrmann, *Phys. Rev. Letters* **20**, 1156 (1968).

<sup>3</sup>R. S. Harp and R. R. Smith, *Phys. Letters* **29A**, 317 (1969).

<sup>4</sup>R. W. Gould, *Phys. Letters* **29A**, 347 (1969).

<sup>5</sup>G. F. Hermann, D. E. Kaplan, and R. M. Hill, *Phys. Rev.* **181**, 829 (1969).

<sup>6</sup>R. M. Hill, D. E. Kaplan, G. F. Herrmann, and S. K. Ichiki, *J. Appl. Phys.* **41**, 929 (1970).

<sup>7</sup>B. D. Guenther, C. R. Christensen, and A. C. Daniel, *Phys. Letters* **30A**, 391 (1969).

<sup>8</sup>P. G. De Gennes, P. A. Pincus, F. Hartmann-Boutron, and J. M. Winter, *Phys. Rev.* **129**, 1105 (1963).

<sup>9</sup>E. L. Hahn, *Phys. Rev.* **80**, 580 (1950).

<sup>10</sup>I. D. Abella, N. A. Kurnit, and S. R. Hartmann, *Phys. Rev.* **141**, 391 (1966).

<sup>11</sup>W. H. Kegel and R. W. Gould, *Phys. Letters* **19**, 531 (1965).

<sup>12</sup>G. F. Herrmann, R. M. Hill, and D. E. Kaplan, *Phys. Rev.* **156**, 118 (1967); G. F. Herrmann and R. F.

Whitmer, *ibid.* **143**, 122 (1966).

<sup>13</sup>R. Weber and M. H. Seavey, *Solid State Commun.* **7**, 619 (1969).

<sup>14</sup>B. D. Guenther, C. R. Christensen, A. C. Daniel, and Peter M. Richards, *Phys. Letters* **33A**, 355 (1970).

<sup>15</sup>Peter M. Richards, *Phys. Rev.* **173**, 581 (1968).

<sup>16</sup>H. Suhl, *Phys. Rev.* **109**, 606 (1958); T. Nakamura, *Progr. Theoret. Phys. (Kyoto)* **20**, 542 (1958).

<sup>17</sup>L. B. Welsh, *Phys. Rev.* **156**, 370 (1967).

<sup>18</sup>R. J. Mahler and L. W. James, *Bull. Am. Phys. Soc.* **12**, 1117 (1967).

<sup>19</sup>H. S. Bennett and P. C. Martin, *Phys. Rev.* **138**, A608 (1965).

<sup>20</sup>D. G. McFadden and R. A. Tahir-Kheli, *Phys. Rev.* **B 1**, 3649 (1970).

<sup>21</sup>M. E. Lines and E. D. Jones, *Phys. Rev.* **139**, A1313 (1965).

<sup>22</sup>G. L. Witt and A. M. Portis, *Phys. Rev.* **136**, A1316 (1964).

<sup>23</sup>G. N. Watson, *A Treatise on the Theory of Bessel Functions* (Cambridge U. P., New York, 1962).

## Direction of the Magnetic Easy Axis in $\gamma'$ -Fe<sub>4</sub>N

J. C. Wood, Jr.\* and A. J. Nozik

American Cyanamid Company, Central Research Division, Stamford, Connecticut 06904

(Received 13 May 1971)

The direction of the easy axis of magnetization in  $\gamma'$ -Fe<sub>4</sub>N has been determined by detailed analysis of certain peaks in the Mössbauer spectrum of a powdered sample in an applied magnetic field. The analysis indicates the magnetic-easy-axis direction to be along  $\langle 100 \rangle$ . The electric field gradient at the face-centered Fe atoms is calculated to be  $-7.0 \times 10^{14}$  esu/cm<sup>3</sup>.

### I. INTRODUCTION

Recent Mössbauer-effect studies<sup>1,2</sup> of  $\gamma'$ -Fe<sub>4</sub>N have shown the existence of two magnetic hyper-

fine patterns for the crystallographically equivalent face-centered iron atoms. These patterns arise because of a difference in the angles between the internal magnetic field and the principal axis of